Modern Pathology (2020) 33:1930–1944
https://doi.org/10.1038/s41379-020-0542-z

ARTICLE

NFATc2-rearranged sarcomas: clinicopathologic, molecular, and cytogenetic study of 7 cases with evidence of AGGRECAN as a novel diagnostic marker

Raul Perret[1] · Julien Escuriol[1,2] · Valérie Velasco[1] · Laetitia Mayeur[1] · Isabelle Soubeyran[1,3] · Christophe Delfour[4] · Sébastien Aubert[5] · Marc Polivka[6] · Marie Karanian[7,8] · Alexandra Meurgey[7] · Sophie Le Guellec[9] · Noelle Weingertner[10] · Sylvia Hoeller[11] · Jean-Michel Coindre[1,2] · Frédérique Larousserie[12] · Gaëlle Pierron[13] · Franck Tirode[8] · François Le Loarer[1,2,3]

Received: 23 November 2019 / Revised: 26 March 2020 / Accepted: 26 March 2020 / Published online: 23 April 2020

Abstract

NFATc2-rearranged sarcomas (*NFATc2*-Sarcomas) are infrequent round cell tumors characterized by *EWSR1-NFATc2* fusions and *FUS-NFATc2* fusions. Although our knowledge on these neoplasms has increased recently, novel diagnostic tools and more comprehensive series are still needed. Here, we describe the features of a series of seven molecularly confirmed *NFATc2*-Sarcomas (*EWSR1-NFATc2*, $n = 4$; *FUS-NFATc2*, $n = 3$) and demonstrate the utility of AGGRECAN immunohistochemistry for their identification. Patients were four males and three females, ranging in age from 19 to 66 years (median: 33). All were primary bone tumors (femur, $n = 4$; tibia, $n = 2$; ilium, $n = 1$), frequently infiltrating the surrounding soft tissues. Treatment often consisted of neoadjuvant chemotherapy and surgery. Follow-up was available for six patients (median 18 months, range 5–102 months), three patients died of disease and four patients are currently alive. Histologically, tumors consisted of monotonous round cells growing in lobules and sheets in variable amounts of fibrous to myxoid stroma. Other findings included spindle cells, corded and trabecular architecture, nuclear pleomorphism, cartilaginous differentiation, and osteoid-like matrix. Histological response to neoadjuvant chemotherapy was poor in all resection specimens available for review ($n = 4$). Tumors were diffusely positive for AGGRECAN and CD99 (7/7), and a subset expressed Pan-Keratin (AE1-AE3; 3/6), S100 (2/6), BCOR (2/6), ETV-4 (2/5), WT1 (2/6), and ERG (2/5). Desmin, NKX3-1, and SATB2 were negative (0/6). Diffuse AGGRECAN staining was also seen in 8/129 round cell sarcomas used for comparison, including mesenchymal chondrosarcoma (7/26) and *CIC*-sarcoma (1/26). Array-CGH showed complex karyotypes with recurrent deletions of tumor suppressor genes (*CDKN2A/B, TUSC7, and DMD)* in three *FUS-NFATC2* cases and a simpler profile without homozygous losses in one *EWSR1-NFATc2* case. Segmental chromosomal gains covering the loci of the fusion genes were detected in both variants. Overall, our study confirms and expands previous observations on *NFATc2*-sarcomas and supports that AGGRECAN is a useful biomarker of these tumors.

Introduction

Small round cell sarcomas comprise a heterogeneous group of tumors of uncertain origin that are diagnostically challenging due to their poorly differentiated morphology. The prototype of these neoplasms is Ewing sarcoma (ES), which is characterized by translocations involving *EWSR1* or rarely *FUS*, and an array of genes of the ETS family of transcription factors (*FLI-1* or *ERG* in >90% of cases) [1]. In 2009, Szuhai K et al. described for the first time a round cell sarcoma with a novel *EWSR1-NFATc2* fusion associated with an unbalanced profile with gains of

These authors contributed equally: Raul Perret, Julien Escuriol

Supplementary information The online version of this article (https://doi.org/10.1038/s41379-020-0542-z) contains supplementary material, which is available to authorized users.

✉ Raul Perret
r.perret@bordeaux.unicancer.fr

✉ François Le Loarer
f.le-loarer@bordeaux.unicancer.fr

Extended author information available on the last page of the article

chromosomes 20q and 22q [2]. Although these cases were initially considered ES variants, subsequently, several clinical and histologic differences have been noted including nested/corded disposition of cells, nuclear atypia, prominent myxoid and hyaline stroma, male predominance, and higher age onset [3–5]. Furthermore, studies using methylome [6], transcriptome [7–9], and copy number analysis [2, 6] have shown distinct profiles in *NFATc2*-rearranged sarcomas (*NFATc2*-Sarcomas), widening the gap with ES.

Recently, our group reported a transcriptional analysis of round cell sarcomas and described three cases with *FUS-NFATc2* fusions [8]. Notably, *NFATc2*-sarcomas clustered in two groups, depending on the involvement of *EWSR1* or *FUS*, and were distinct from all other round cell sarcomas, including ES, *CIC*-rearranged sarcomas, *BCOR*-rearranged sarcomas, and myoepithelial tumors. Also, gene expression analysis evidenced AGGRECAN as a potential diagnostic candidate in both *NFATc2* clusters.

Since the original description, several cases of *NFATc2*-Sarcoma have been reported, but due to their infrequency, these neoplasms remain poorly characterized. Furthermore, useful immunohistochemical markers for their distinction from potential mimics are scarce. In the present study, we describe the clinicopathological, molecular, and cytogenetic findings of seven cases of *NFATc2*-Sarcoma and validate the diagnostic utility of AGGRECAN as an immunohistochemical marker for identifying these tumors. Further, we reviewed the literature and discussed the clinical findings of all reported cases to date.

Materials and methods

Case selection

Cases of small round cell sarcomas harboring *NFATc2* rearrangements were retrieved from the French Sarcoma Network database (RRePS). This directory is approved by the National Committee for Protection of Personal Data (CNIL, no 910390), in alignment with the ethical principles of the Helsinki Declaration. A further case was provided by the University Hospital of Basel (Switzerland). A total of seven cases were found, which included six resection specimens (cases 1, 2, 3, 4, 5, and 7) and one biopsy (case 6). Two specimens (cases 2 and 3) were the subject of a previous study [8]. Clinically relevant data, medical imaging, and macroscopic findings were recovered from the referring centers and the French clinical reference network for soft tissue and visceral sarcomas (NETSARC) database.

Immunohistochemical screening with AGGRECAN in round cell sarcomas

Considering the results of gene expression profiling showing an enriched expression of *ACAN* in *NFATc2*-Sarcoma [8], we performed a screening of a large group of tumors with an antibody targeting the gene's product AGGRECAN. Immunohistochemical expression was assessed in 129 cases of small round cell tumors, which included: 58 ES, 26 mesenchymal chondrosarcomas, 19 *BCOR*-rearranged sarcomas, and 26 *CIC*-rearranged round cell sarcomas. Also, a group of 35 tumors presenting a prominent cartilaginous, myxoid or osteoid matrix was selected for testing, including 2 primary bone chondrosarcomas, 8 chordomas, 10 myoepithelial tumors, 1 angiofibroma of soft tissue and 14 osteosarcomas (1 low-grade central and 13 conventional, including 3 with chondroblastic areas). Expression in the normal background tissues included in the studied slides and normal samples from colorectal, thyroid, bone marrow, and tonsil tissue was also evaluated.

Immunostaining

Immunohistochemistry was performed on four micrometers paraffin sections as per standard technique on a Ventana Benchmark ULTRA automat (Ventana, Roche Diagnostics) using the antibodies listed in Table 1. The type of expression was assessed (membranous, cytoplasmic, perinuclear), and its extent was graded as negative (no expression or expression <5% tumor cells); focally positive (5–90%) and diffusely positive (>90%).

Fluorescence in situ hybridization

Fluorescence in situ hybridization (FISH) analysis was performed on interphase nuclei from 4 µm-thick sections of formalin-fixed paraffin-embedded (FFPE) tissue. The following commercial probes were used: *EWSR1* Break-Apart probe (Case 1: Vysis LSI *EWSR1* (22q12) Dual Color Break Apart Rearrangement Probe, Abbot, reference: 00884999029125. Cases 5 and 7: ZytoLight SPEC *EWSR1* Dual Color Break Apart Probe, ZytoVision, reference: Z-2096-50×4. Case 6: Agilent SureFISH *EWSR1* 5′ BA 564 kb, reference: G101077G-8; Sure FISH *EWSR1* 3′ BA 263 kb, reference: G101076R-8), FUS Break-Apart probe (Case 2: ZytoLight SPEC *FUS* Dual Color Break Apart Probe, Zytovision, reference Z-2130-50). Nuclei were scored for non-rearranged patterns (red and green fusion signals), rearranged, and unbalanced patterns (split of red and green signals or extra single red/green signals). At least 50 non-overlapping intact nuclei were counted, and the positive cut-off to call the FISH assay positive was 20%.

Table 1 Immunohistochemical antibodies and staining protocol.

Antibody	Manufacturer	Clone	Concentration	Pretreatment	Incubation time /detection
BCOR	Santa Cruz Sc-514576	C-10	1/50	CC2 (56′)	60′/OptiView universal DAB
CD99,MIC2	Dako, Glostrup, Danemark (M3601)	12E7	1/100	CC1 short (36′)	32′/UltraView universal DAB
Pan-Keratin	Roche Diagnostics (760-2595)	(AE1/AE3/PCK26)	Prediluted	CC1 short (36′) + Protéase3(4′)	8′/UltraView universal DAB
Desmin	Roche Diagnostics (760-2513)	DE-R-11	Prediluted	CC1 short (36′)	32′/ UltraView universal DAB
ERG	Dako, Glostrup, Danemark (M7314)	EP111	1/100	CC1 short (36′)	32′/ UltraView universal DAB
PEA3-ETV4	Santa Cruz Sc-113	16	1/25	CC1 standard (64′)	32′/OptiView universal DAB + amplification (8’)
PS100	Dako, Glostrup, Danemark (Z 311)	Rabbit polyclonal	1/2000	CC1 (20′)	32′/UltraView universal DAB
WT1-cTer	Zytomed Systems GmbH 14163 Berlin, Germany (523-3994)	Rabbit polyclonal	1/100	CC1 standard (64′)	32′/UltraView universal DAB
NKX3-1	Bio SB 93111 Santa Barbara, CA, USA	EP356 (CE/IVD) Rabbit monoclonal	Prediluted	CC1 (48 min)	36′/OptiView universal DAB
AGGRECAN	Abcam (ab186414)	EPR14664	1/1000	CC1 standard (64′)	52′/UltraView universal DAB

Whole RNA-sequencing and hierarchical cluster analysis

Whole RNA-sequencing was performed in all seven cases. FFPE was employed in six cases (cases 1, 2, 3, 4, 5, and 7) and frozen material in one case (case 6). Studies using FFPE material were performed as previously described [10]. Briefly, total RNAs were isolated from FFPE tissue section using the Formapure RNA kit (Beckman Coulter, Brea, CA). Library constructions were performed using the Tru-Seq RNA Access Library Prep Kit (Illumina, San Diego, USA). Sequencing was performed on the NextSeq 500 Sequencing System (Illumina, San Diego, USA). For fusion transcript detection, sequencing reads were analyzed with Defuse, Starfusion and FusionMap tools using hg19 genome as a reference. The RNA sequencing with frozen material from case 6 was performed as previously described [8]. To perform cluster analysis, the RNA values of the six FFPE cases were compared with a dataset of sarcomas with round cell morphology which included two additional cases of *NFATc2*-Sarcoma (EWSR1, $n = 1$ and FUS $n = 1$) for which slides where unavailable for review. Gene expression data was extracted using Kallisto v0.42.5 tool [11] with GENECODE release 23 genome annotation based on GRCh38 genome reference. Clustering was performed with the R package Cluster v2.0.3 ConsensusClusterPlus v1.46 [12].

Array-comparative genomic hybridization

Genomic DNA was extracted from FFPE using a commercially available kit (QIAamp® DNA FFPE Tissue Kit; QIAGEN). DNA was hybridized onto 8×60 K whole-genome arrays (G4450A; Agilent Technologies) according to the manufacturer’s protocol (https://www.agilent.com/cs/library/usermanuals/public/G4410-90010_CGH_Enzymatic_7.5.pdf). Microarray slides were scanned using a DNA Microarray Scanner; images were analyzed by Feature Extraction V10.1.1.1, followed by Agilent Cytogenomics software 4.0.3.12. DNA copy number anomalies were interpreted as previously described [13]. A low-level copy number gain was defined as a log 2 ratio > 0.25, and a copy number loss was defined as a log 2 ratio < −0.25. A homozygous deletion was suspected when the ratio was < −1. The range for derivative log ratio spread cut-off was fixed to 0.50. The genomic index (GI) was calculated as follows: genomic index $= A^2/C$, where A is the number of alterations (segmental gains and losses) and C is the number of involved chromosomes [13, 14].

Statistical analysis

The specificity and sensitivity of AGGRECAN staining for *NFATc2*-Sarcoma were assessed by the Fisher’s exact test using GraphPad Prism 6.01 (GraphPad Software, La Jolla, CA, USA). A value of $P < 0.01$ was considered statistically significant. For this analysis, the expression of AGGRECAN in *NFATc2*-sarcomas was compared with the screening group of small round cell sarcomas ($n = 129$).

Results

Clinical findings

Clinical data are summarized in Table 2. Affected patients comprised four males and three females, ranging from 19 to 66 years old (median: 33, mean: 39). All were primary

Table 2 Clinical and pathological features of previously reported and current cases of NFATc2-rearranged sarcomas.

Study	Case	Fusion variant (exon)	Age/sex	Location	Size (cm)	Local recurrence (months)	Metastatic disease	Main treatment	Follow-up (months)/ Vital status
Current[a]	1	$EWSR1_{(8)}$-$NFATc2_{(3)}$	27/M	Tibia	8	No	No	nCT (VDC/IE) + Surgery	102/AWOD
	2	$FUS_{(6)}$-$NFATc2_{(3)}$	33/M	Femur	9	Yes (9,15)	Yes	nCT (API/AI) + Surgery	25/DOD
	3	$FUS_{(6)}$-$NFATc2_{(3)}$	43/M	Femur	15.5	No	Yes	Surgery	7/DOD
	4	$FUS_{(6)}$-$NFATc2_{(3)}$	66/F	Femur	14	Yes (4)	Yes	Surgery	32/DOD
	5	$EWSR1_{(8)}$-$NFATc2_{(3)}$	28/F	Tibia	9.5	No	No	nCT (API/AI) + Surgery	5/AWOD
	6	$EWSR1_{(8)}$-$NFATc2_{(3)}$	19/F	Ilium	18	–	No	nCT (VIDE) + RT	8/AWD
	7	$EWSR1_{(6)}$-$NFATc2_{(3)}$	58/M	Femur	10.5	–	No	nCT (EURO-B.O.S.S) + surgery	Recent case
Yoshida et al. [15]	8	EWSR1-NFATc2	39/M	Femur	NR	NR	NR	NR	NR
	9	EWSR1-NFATc2	46/M	Femur	NR	NR	NR	NR	NR
	10	EWSR1-NFATc2	27/M	Retroperitoneum	NR	NR	NR	NR	NR
	11	EWSR1-NFATc2	31/F	Scapula	NR	NR	NR	NR	NR
	12	EWSR1-NFATc2	36/M	Neck	NR	NR	NR	NR	NR
	13	EWSR1-NFATc2	51/M	Forearm	NR	NR	NR	NR	NR
	14	EWSR1-NFATc2	78/F	Tibia	NR	NR	NR	NR	NR
	15	EWSR1-NFATc2	38/M	Thigh	NR	NR	NR	NR	NR
	16	EWSR1-NFATc2	44/M	Thigh	NR	NR	NR	NR	NR
	17	EWSR1-NFATc2	36/F	Fibula	NR	NR	NR	NR	NR
	18	EWSR1-NFATc2	62/F	Femur	NR	NR	NR	NR	NR
	19	FUS -NFATc2	49/M	Femur	NR	NR	NR	NR	NR
Diaz-Perez et al. [5]	20	EWSR1-NFATc2	28/M	Tibia	4.2	No	No	nCT (ES regimen) + RT + Surgery	144/AWOD
	21	EWSR1-NFATc2	39/M	Femur	14.5	No	No	nCT (ES regimen) + RT + Surgery	30/AWOD
	22	FUS-NFATc2	28/M	Humerus	18	No	No	nCT (ES regimen) + RT	Recent case
	23	EWSR1-NFATc2	46/M	Femur	13.4	Yes (5.9)	Yes	nCT (ES regimen) + RT + Surgery	5.9/AWD
Wang et al. [3]	24	$EWSR1_{(7)}$-$NFATc2_{(3)}$	67/M	Radius	NR	No	No	nCT (VAC/IE) + Surgery	14/AWOD
	25	$EWSR1_{(7)}$-$NFATc2_{(3)}$	32/M	Periclavicular (soft tissue)	NR	No	No	nCT (VAC/IE) + RT + Surgery	24/AWOD
	26	$EWSR1_{(7)}$-$NFATc2_{(3)}$	42/M	Radius	NR	No	Yes	nCT (VAC/IE) + Surgery	16/AWD
	27	$EWSR1_{(7)}$-$NFATc2_{(3)}$	24/F	Gastrocnemius muscle	4	No	No	nCT (VAC/IE) + Surgery	23/AWOD
	28	$EWSR1_{(7)}$-$NFATc2_{(3)}$	42/M	Radius	NR	No	Yes	nCT (VAC/IE) + Surgery	93/DOD
	29	$EWSR1_{(7)}$-$NFATc2_{(3)}$	59/M	Periclavicular (soft tissue)	NR	Yes (6)	No	nCT (VAC/IE) + RT + Surgery	144/AWOD
Koelsche et al.[b] [6]	30	EWSR1-NFATc2	51/M	Humerus	NR				
	31	$EWSR1_{(8)}$-$NFATc2_{(3)}$	39/M	Humerus	NR				
	32	$EWSR1_{(8)}$-$NFATc2_{(3)}$	56/F	Femur	NR	Yes (24) ($n = 1$) No ($n = 2$)	Yes ($n = 1$) No ($n = 2$)	nCT + Surgery ($n = 3$)	NA/AWOD ($n = 1$) 72/Alive ($n = 1$) 24/Alive ($n = 1$)
	33	$EWSR1_{(8)}$-$NFATc2_{(3)}$	16/M	Femur	NR				
	34	$EWSR1_{(8)}$-$NFATc2_{(3)}$	17/F	Humerus	NR				

Table 2 (continued)

Study	Case	Fusion variant (exon)	Age/sex	Location	Size (cm)	Local recurrence (months)	Metastatic disease	Main treatment	Follow-up (months)/ Vital status
Mantilla et al. [16]	35	EWSR1-NFATc2	67/M	Thigh (muscle)	NR	NR	NR	Surgery	Lost
Bode-Lesniewska et al. [4]	36	EWSR1-NFATc2	34/F	Femur	NR	No	Yes	nCT (MAP) + Surgery	132/AWOD
	37	EWSR1-NFATc2	42/M	Tibia	NR	No	No	Surgery	102/AWOD
	38	EWSR1-NFATc2	60/F	Intra-abdominal	NR	No	No	Surgery	8/AWOD
	39	FUS-NFATc2	12/M	Humerus	NR	No	No	Surgery (curettage)	8/AWOD
Yau et al. [17]	40	$EWSR1_{(7)}$-$NFATc2_{(3)}$	43/M	Femur	8.5	No	No	RT, nCT (IVADo) + Surgery	12/AWOD
Watson et al. [8]	41	FUS-NFATc2	49/F	Femur	NR	NR	NR	NR	NR
	42	EWSR1-NFATc2	32/M	Humerus	NR	NR	NR	NR	NR
	43	EWSR1-NFATc2	12/F	Tibia	NR	NR	NR	NR	NR
	44	EWSR1-NFATc2	61/M	Calf	NR	NR	NR	NR	NR
	45	EWSR1-NFATc2	23/M	Femur	NR	NR	NR	NR	NR
Toki et al. [18]	46	EWSR1	NR	NR	NR	NR	NR	NR	NR
Antonescu [19]	47	EWSR1-NFATc2	42/M	Femur	NR	NR	NR	NR	NR
Machado et al. [20]	48	EWSR1-NFATc2	NR	Fibula	NR	NR	NR	NR	NR
Cohen et al. [21]	49	$EWSR1_{(10)}$-$NFATc2_{(3)}$	24/F	Calf (soft tissue)	6	No	No	nCT (VAC/IE) + Surgery	12/AWOD
Brohl et al. [25]	50	$FUS_{(6)}$-$NFATc2_{(9)}$	15/M	Femur	NR	NR	NR	NR	NR
Kinkor et al. [22]	51	$EWSR1_{(9)}$-$NFATc2_{(4)}$	12/M	Femur	7	No	No	nCT + Surgery	11/AWOD
	52	$EWSR1_{(9)}$-$NFATc2_{(4)}$	28/M	Humerus	NR	Yes	Suspicious lung	Surgery + metastatic CT	53/AWD
Sadri et al. [23]	53	$EWSR1_{(8)}$-$NFATc2_{(3)}$	30/M	Femur	8.3	Yes (30)	No	Surgery + CT	36/AWOD
Romeo et al. [24]	54	EWSR1	32/M	Bone (lower extremity)	NR	NR	No	NR	64/AWOD
Szuhai et al. [2]	55	$EWSR1_{(8)}$-$NFATc2_{(3)}$	21/M	Thigh	NR	NR	NR	NR	NR
	56	$EWSR1_{(8)}$-$NFATc2_{(3)}$	25/M	Femur	NR	NR	NR	NR	NR

AWOD alive without disease, *AWD* alive with disease, *DOD* dead of disease, *M* male, *F* female, *NR* not reported, *ES* ewing sarcoma, *RT* radiotherapy, *nCT* neoadjuvant chemotherapy, *CT* chemotherapy, *API-AI* doxorubicin, cisplatin, ifosfamide, mesna, and lenograstim, *VIDE* vincristine, ifosfamide, doxorubicin, and etoposide, *IVADo* ifosfamide, vincristine, actinomycin D and doxorubicin, *MAP* cisplatin, doxorubicin, methotrexate, *EURO-B.O.S.S* cisplatin, adriamycin, and ifosfamide (only preoperative scheme had been performed at the time of this study).

[a]Two cases from this series were originally reported in the study of Watson et al.

[b]Two cases from this series were originally published in the study by Szuhai et al. [2].

bone tumors ranging in size from 8 cm to 18 cm (median: 10.5 cm; mean: 12.07 cm). Six cases were located in the long bones (femur, $n = 4$; tibia, $n = 2$) and one case was located in the ilium. Radiologically, all lesions were described as lytic, and most (6/7) infiltrated the surrounding tissues (Fig. 1).

Complete surgical excision with negative margins was performed in 6/7 cases. The remaining patient (case 6) was exclusively treated with chemotherapy and radiotherapy due to inoperable disease. Neoadjuvant chemotherapy was performed in 5/7 cases (cases 1, 2, 5, 6, and 7). ES chemotherapy regimen was administered in two cases and consisted of VDC/IE (alternating Vincristine, Doxorubicin, Cyclophosphamide, and Ifosfamide, Etoposide) in case 1 and VIDE (Vincristine, Ifosfamide, Doxorubicin, and Etoposide) in case 6. Osteosarcoma chemotherapy with API-AI (Doxorubicin, Cisplatin, ifosfamide, Mesna, and Lenograstim) regimen was administered in cases 2 and 5. Neoadjuvant chemotherapy according to the EURO-B.O.S.S. protocol (Cisplatin, Adriamycin, and Ifosfamide), was administered in case 7. One patient (case 2) was treated with suboptimal doses due to chemotherapy-related toxicity. One patient (case 1) was treated with postoperative radiotherapy 4 months after surgery. At the time of this study, the patient solely treated with chemotherapy and radiotherapy (case 6) was receiving the sixth cycle of neoadjuvant chemotherapy with no objective response on radiological follow-up imaging.

Clinical follow-up was available for six cases (median: 18 months, mean: 27 months, range: 5–102 months). One case (case 7) was recently diagnosed. Local recurrences occurred in two cases (cases 2 and 4), and both subsequently underwent amputation of the lower extremity. Three cases developed metastatic disease. One patient (case 4) had lung metastases at the time of diagnosis. One patient (case 2) developed metastatic disease to the lungs 19 months after the initial diagnosis and subsequent lymph node spread (inguinal and iliac). For the remaining patient (case 3), the topography and time of metastasis were unknown. Three patients (cases 2, 3, and 4) died of disease; Three patients (cases 1, 5, and 7) are alive without disease, and one patient (case 6) is alive with disease.

Pathological findings

Among the six cases where a surgical excision was performed, gross examination revealed relatively well circumscribed and lobulated gray-white fleshy masses with variably necrotic and hemorrhagic areas (Fig. 1). Further, most cases had a large extra-osseous component.

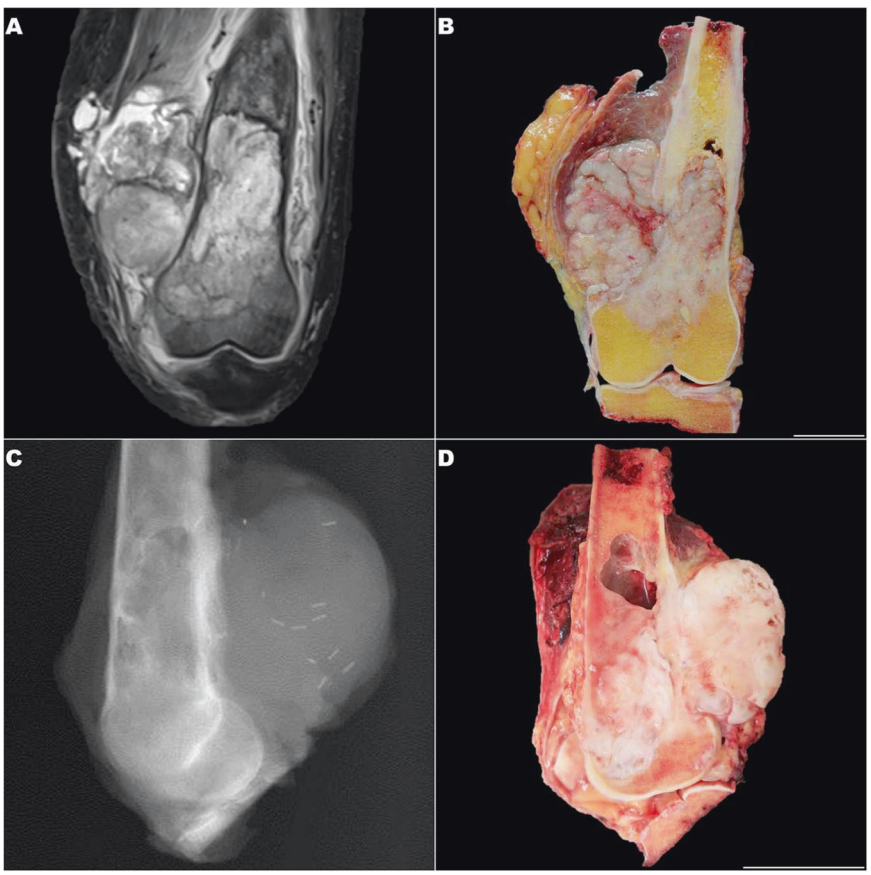

Fig. 1 Imaging and gross findings of *NFATc2*-rearranged sarcomas. **a**, **b** (case 4), magnetic resonance imaging with STIR (Short tau inversion recovery) showing a large tumor replacing the medullary cavity of the distal femur associated with a massive extra-osseous component. Grossly, the tumor was a large fleshy mass with hemorrhagic areas and multilobular contours. **c**, **d** (case 7), radiograph of the surgical specimen showing an ill-defined lytic mass growing posteriorly into the soft tissues. Grossly, the tumor manifested as a large destructive fleshy mass breaking through the cortex and invading the surrounding tissues, note the marked periosteal reaction. Scale bars 5 cm.

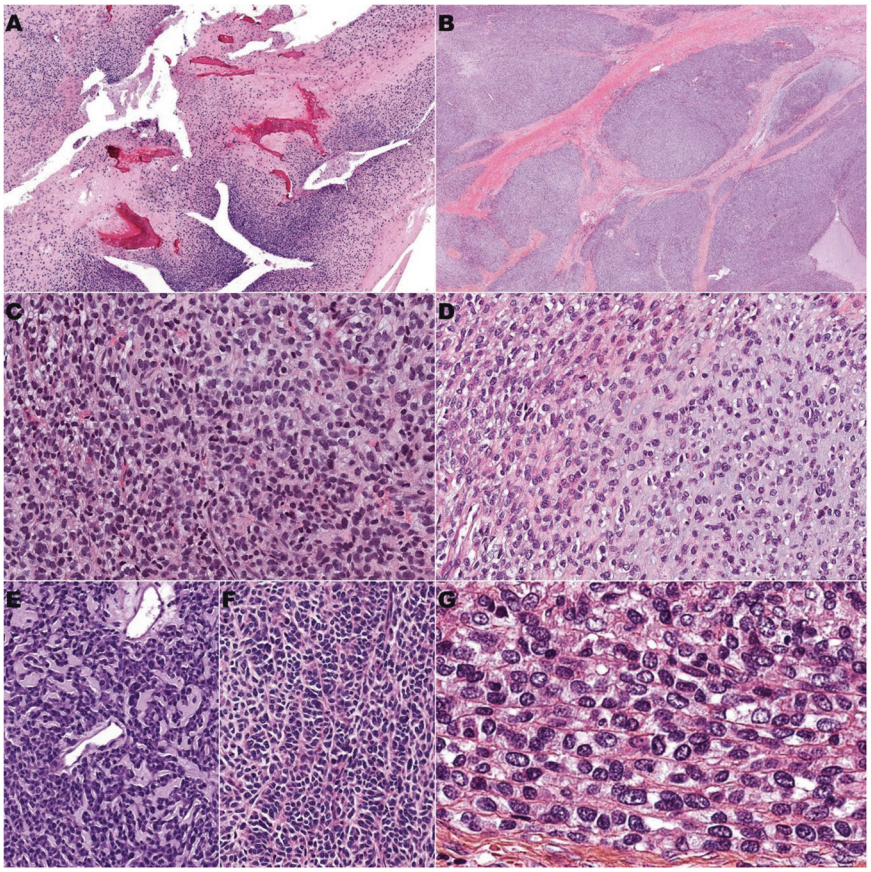

Fig. 2 Morphological spectrum of *NFATc2*-rearranged sarcomas. a (Case 2), an intramedullary portion of a tumor showing massive permeation of the bone marrow space. **b** (Case 4), low-magnification view showing a lobulated growth pattern, a frequent feature present in most tumors. **c**, **d** (Cases 6 and 4, respectively), high-magnification reveals typical morphological features consisting of sheets of monotonous round cells within variable amounts of intervening stroma, ranging from scant (**c**) to abundant and myxoid (**d**, right area of the image). **e**, **f** (Cases 2 and 3, respectively), in some cases, tumor cells were focally arranged in cords (**e**) and trabeculae (**f**), the latter reminiscent of a neuroendocrine neoplasm. **g** (Case 3), high-power image showing tumor cells with round and irregular nuclei surrounded by a fibrous stroma consisting of thin strands of collagen.

Initially, three cases had been classified as *NFATc2*-rearranged sarcoma (Cases 1, 6, and 7) while four cases were referred for consultation with the following diagnoses: round cell sarcoma (Case 3), high-grade sarcoma (Case 4), round cell osteosarcoma (Case 5), and osteosarcoma with chondroblastic differentiation (Case 2). Histologically, the tumors massively infiltrated the pre-existent bone (Fig. 2a) and consisted of lobules and sheets of monotonous round cells within a variably abundant fibrous to myxoid stroma (Fig. 2b–d). Tumor cell nuclei were round to oval, and chromatin was fine to vesicular with fairly prominent nucleoli. The cytoplasm was scant or moderately abundant and eosinophilic to pale. In a subset of cases, tumor cells were arranged in cords or trabeculae (Fig. 2e, f). Mitotic activity was high (>20/10 HPF) in three tumors (cases 2, 3, and 4) and low (<5/10 HPF) in the four remaining cases. Delicate interstitial fibrosis frequently surrounding tumor nests and individual cells was a frequent feature (Fig. 2g). In four tumors (cases 2–5), large areas of coagulative necrosis were present, and in three of these cases (cases 2, 3, and 4), necrosis respected the neoplastic cells surrounding central blood vessels (peritheliomatous necrosis). Spindle-shaped cells were focally present in most tumors, but they were predominant in case 7 (Fig. 3a, b). Other findings included cartilaginous differentiation in three cases (cases 2, 3, and 7, Fig. 3c, d), a prominent collagenous matrix simulating osteoid in 1 case (case 5, Fig. 3e) and pleomorphic cells in 2 cases (cases 2 and 3; Fig. 3c, f). Of note, the presence of cartilaginous and osteoid-like matrix in cases 2 and 5 derived in their initial misclassification as osteosarcomas. In the four neoplasms treated with both neoadjuvant chemotherapy and surgical excision (cases 1, 2, 5, and 7), pathology reports described <90% of necrosis/fibrosis (range: 0–80%).

Immunohistochemistry

The immunohistochemical profiles are detailed in Table 3. All cases showed diffuse cytoplasmic expression of AGGRECAN (Fig. 4a, b). Similarly, CD99 was diffusely positive in all samples, but the staining was cytoplasmic (paranuclear dot-like) in four cases and membranous in three cases (Fig. 4c, d). Focal Pan-Keratin expression was seen in 3/6 cases (Fig. 4e). Focal nuclear BCOR and ETV-4 staining were seen in 2/6 cases and 2/5 cases, respectively. Nuclear WT1 staining was present in 2/6 cases, ranging from focal to diffuse. Focal nuclear ERG expression was seen in 2/5 cases. PS100 was negative in the round cell component of the six tested cases and was diffusely expressed in the chondroid areas of two cases (cases 3 and

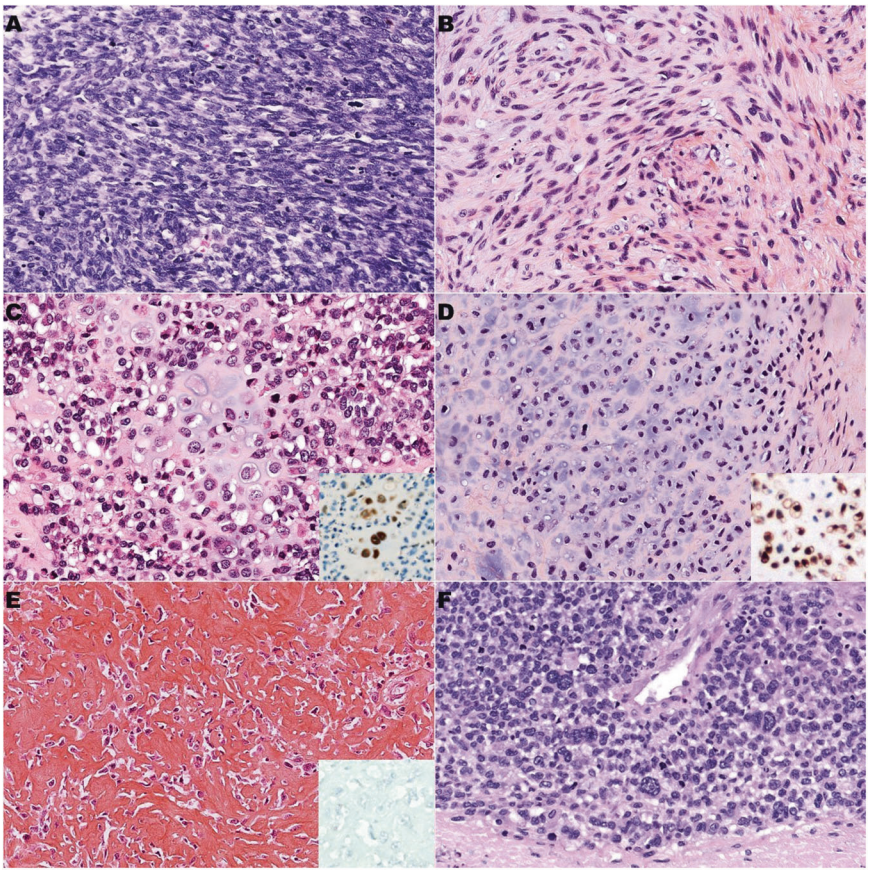

Fig. 3 Morphological spectrum of *NFATc2*-rearranged sarcomas. a (Case 2), high-power view showing spindle cells, a focal finding seen in most tumors. **b** (case 7), a single tumor was predominantly composed of spindle cells in an abundant fibrous to myxoid matrix. **c**, **d** (Cases 3 and 7, respectively), high-power shows abrupt cartilaginous differentiation, which was present in a subset of tumors. Pleomorphic cells were seen in some of these regions (**c**). PS100 positivity (insets) suggests the presence of true cartilaginous differentiation. **e** (Case 5), a single tumor had a prominent collagenous matrix (osteoid-like) closely mimicking osteoblastic osteosarcoma; SATB2 was completely negative in these areas (inset). **f** (Case 2), High-power image depicts pleomorphic cells present in areas without cartilaginous differentiation.

Table 3 Immunohistochemical profile of *NFATc2*-sarcomas.

Case	CD99	Pan-Keratin	Desmin	S100	BCOR	WT1	ETV4	SATB2	ERG	NKX3-1	AGGRECAN
1	+ (membranous)	–	–	–	–	–	–	–	–	–[a]	+
2	+ (paranuclear dot-like)	–	–	–	–	±	–	–	–	–	+
3	+ (paranuclear dot-like)	–[a]	–	±[b]	±	+	±	–	–	–[a]	+
4	+ (paranuclear dot-like)	±	–	–	±	–	±	–	±	–	+
5	+ (membranous)	–	–	–	–	–	–	–	NP	–	+
6	+ (membranous)	NP	NP	NP	NP	NP	NP	–	NP	NP	+
7	+ (paranuclear dot-like)	±	–	±[b]	–	–	NP	NP	±[b]	–	+

Extent of expression: – (no expression or expression <5% tumor cells); ± (5–90% positive cells); + (>90% positive cells).

NP not performed.

[a]Expression in isolated cells.

[b]Expression in cartilaginous areas.

7). The following markers were negative: NKX3-1 ($n = 6$), Desmin ($n = 6$), and SATB2 ($n = 6$).

Landscape of staining reactivity with AGGRECAN

Staining patterns of all screened cases are summarized in Table 4. The sensitivity and specificity of any degree of AGGRECAN staining (focal or diffuse) were 100% (95% CI, 59–100%) and 76% (95% CI, 68–83%), respectively. Moreover, diffuse staining showed a sensitivity and specificity of 100% (95% CI, 59–100%) and 93% (95% CI, 88–97%), respectively. This type of expression was rare in the small round cell control group and included mesenchymal chondrosarcomas (7/26, 28%) and *CIC*-sarcomas (1/26, 4%). In the cohort of tumors presenting a prominent cartilaginous, myxoid or osteoid matrix, AGGRECAN was diffusely expressed in 8/8 chordomas, 2/2 chondrosarcomas, 5/14 osteosarcomas (including the three cases with chondroblastic areas) and 3/10 myoepitheliomas of soft tissue. Finally, AGGRECAN staining was

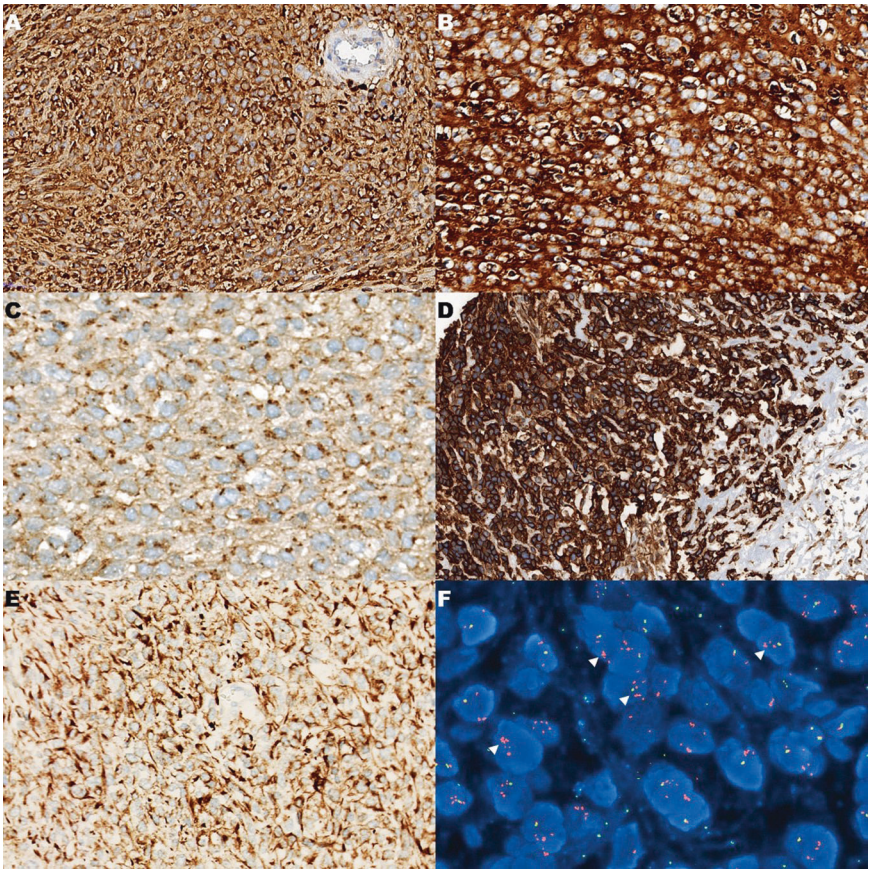

Fig. 4 Immunohistochemical and fluorescence in situ hybridization (FISH) findings in *NFATc2*-rearranged sarcomas. a, **b** (cases 4 and 2, respectively), cytoplasmic staining of AGGRECAN was strong and diffuse in all samples. **c**, **d** (cases 4 and 5, respectively), CD99 was expressed in all tumors, but staining varied from cytoplasmic dot-like (**c**) to membranous (Ewing Sarcoma pattern, **d**). **e** (Case 4), Cytoplasmic Pan-Keratin expression was present in three cases. **f** (Case 1), FISH analysis using *EWSR1* break-apart probes, showing gains of the 5′ probe stained in red (arrowheads) but only two copies of the 3′ probe in green, suggestive of an unbalanced translocation.

Table 4 AGGRECAN staining in 164 sarcomas and soft tissue neoplasms.

Tumor Subtype ($n = 164$)	Type of staining		
	Negative	Focally positive	Diffusely positive
Ewing sarcoma (58)	54 (93%)	4 (7%)	0
Mesenchymal chondrosarcoma (26)	3 (11%)	16 (61%)	7 (28%)
BCOR sarcoma (19)	19 (100%)	0	0
CIC sarcoma (26)	23 (88%)	2 (8%)	1 (4%)
Soft tissue myoepithelioma (10)	4 (40%)	3 (30%)	3 (30%)
Angiofibroma of soft tissue (1)	1 (100%)	0	0
Chordoma (8)	0	0	8 (100%)
Chondrosarcoma (2)	0	0	2 (100%)
Osteosarcoma (14)	1 (7%)	8 (57%)	5 (36%)

Extent of tumor cell staining: negative (no expression or expression in <5%); focally positive (5–90%); diffusely positive (>90%).

only noted in normal vascular walls and mature cartilage (both normal and neoplastic), the rest of the analyzed tissues were negative.

FISH analysis

FISH analysis was performed in five cases (cases 1, 2, 5, 6, and 7). Studies showed rearrangement of *EWSR1* in all *EWSR1-NFATc2* cases with gains of the 5′ portion of the probe (suggestive of an unbalanced translocation) in 3/4 cases (cases 1, 5, and 6; Fig. 4f). In case 7, gains of both the 5′ and 3′ portions of the *EWSR1* probe were detected. Similarly, an unbalanced pattern with signal gains of the 5′ portion of the *FUS* gene was seen in the single tested case with a *FUS-NFATc2* fusion (case 2).

RNA sequencing findings

Results demonstrated fusions involving exon 8 of *EWSR1* and exon 3 of *NFATc2* in three cases (cases 1, 5, and 6); exon 6 of *EWSR1* and Exon 3 of *NFATc2* in one case (case 7) and exon 6 of *FUS* and exon 3 of *NFATc2* in three cases (cases 2, 3, and 4). Additional translocations were detected in two cases. Case 4 harbored a *PCSK6-FUS* fusion and case 7 a *CREBBP-PMM2* fusion. Unsupervised cluster analysis showed that both *FUS* and *EWSR1* variants formed common clusters, independent of other sarcoma subtypes (Supplementary Material).

Array-based comparative genomic hybridization findings

A summary of the main chromosomal aberrations of the four tested cases (cases 1–4) is shown in Table 5. The three cases with *FUS-NFATc2* fusions (cases 2–4) showed complex chromosome profiles with high genomic indices while the single tested case harboring an *EWSR1-NFATc2* fusion had a simpler profile (Fig. 5). All three neoplasms with *FUS-NFATc2* fusions presented homozygous deletions of 9p21.3 (including *CDKN2A* and *CDKN2B)*. Besides, losses of 3q13.31 (including *TUSC7*) and Xp21 (including *DMD)* were seen in three (cases 2, 3, and 4) and two cases (cases 2 and 3), respectively. Segmental gains of chromosome 20q covering *NFATc2* loci were seen in two cases (cases 1 and 2). Moreover, case 1 had a segmental gain of chromosome 16p spanning *FUS* locus, and case 2 had a segmental gain of chromosome 22q including *EWSR1* locus. Whole chromosome gain of chromosome 8 was seen in two cases (cases 1 and 2). Genomic breakpoints within the *NFATc2, EWSR1*, and *FUS* loci were identified in three cases (cases 1, 2 and 3), one case (case 1), and one case (case 2), respectively. In case 3, the assessment of a *FUS* breakpoint was equivocal due to insufficient probe coverage. Finally, a heterozygous loss of chromosome 9q was identified in a single case (case 1).

Discussion

We herein characterized a group of seven round cell sarcomas harboring *NFATc2* rearrangements and demonstrated for the first time that they consistently express AGGRECAN. When considering all reported cases with clinical information [2–6, 8, 15–25] (Table 2), these tumors show a male predominance (Male:Female ratio 2.6:1) and mainly affect adults in their late 30s (median and mean: 37 and 38 years old, respectively). Most reported cases developed in the long tubular bones, particularly the femur and humerus, but several cases have been reported in extra-osseous locations [3, 4, 15, 16, 21]. Imaging studies from skeletal tumors frequently show large lytic lesions transgressing the cortical bone and forming large soft-tissue masses.

Reported disease prognosis has been somewhat variable among studies [3, 4, 6]. In our series, almost half of the neoplasms had aggressive clinical behavior, which included local recurrence, metastatic spread, and patient's death. Overall, when considering current data of all cases with available follow-up, local recurrence or metastasis has been reported in 42% of *NFATc2*-Sarcomas (12/28 cases, Table 2). These results suggest a roughly similar clinical course with skeletal ES where the reported relapse rate is between 30 and 40% [26–28]. Notably, although aggressive

Table 5 Summary of main genomic alterations detected by Array-based Comparative Genomic Hybridization.

Case	Genomic index	Homozygous loss (gene)	Gain (gene)	Fusion gene breakpoints (genomic coordinates[a])	Other findings
Case 1	28.8	–	7; 8; 20q13.12; 20q13.13-13.2; 22q11.1-q12.1; 22q12.1-q12.2	- *NFATc2* (20:50,112,183-50,157,437) - *EWSR1*: (22:29,673,668-29,682,794)	-Heterozygous loss of 9q
Case 2	62.5	9p21.3 (*CDKN2A/CDKN2B*); interstitial loss of Xp21 (*DMD*); 3q13.31 (*TUSC7*)	3q13.31-qter; 4q; 8; 20p; 20q11.21-q13.2 (including *NFATc2*); 16p13.3-p11.2 (including *FUS*)	- *NFATc2* (20:50,112,183-50,157,437) - *FUS* (16:31,196,228-31,227,791)	–
Case 3	344	2p12 (including *CTNNA2*); 9p21.3 (*CDKN2A/CDKN2B*); Xp21.2; Xp11.4-p11.3; Xq21.33-q28; Xp22.33-p22.2; 3q13.31 (*TUSC7*)	8q21.11; 12p13.33-p13.1; 12q15 (including *MDM2*)	- *NFATc2* (20:50,007,988-50,157,437)	-Heterozygous loss of Xp21 (including *DMD*)
Case 4	103	9p24.3; 9p21.3-p21.1; 9p21.3 (*CDKN2A/CDKN2B*); 14q21.2; Xq23	8p11.21-p11.1; 8q11.1-q24.3; 9p24.3-p22.2 (including SMARCA2); 18q12.1 (including *CDH2*);	–	Heterozygous loss of 3q13.31 (TUSC7)

[a]Based on Genome Reference Consortium Human Build 37.

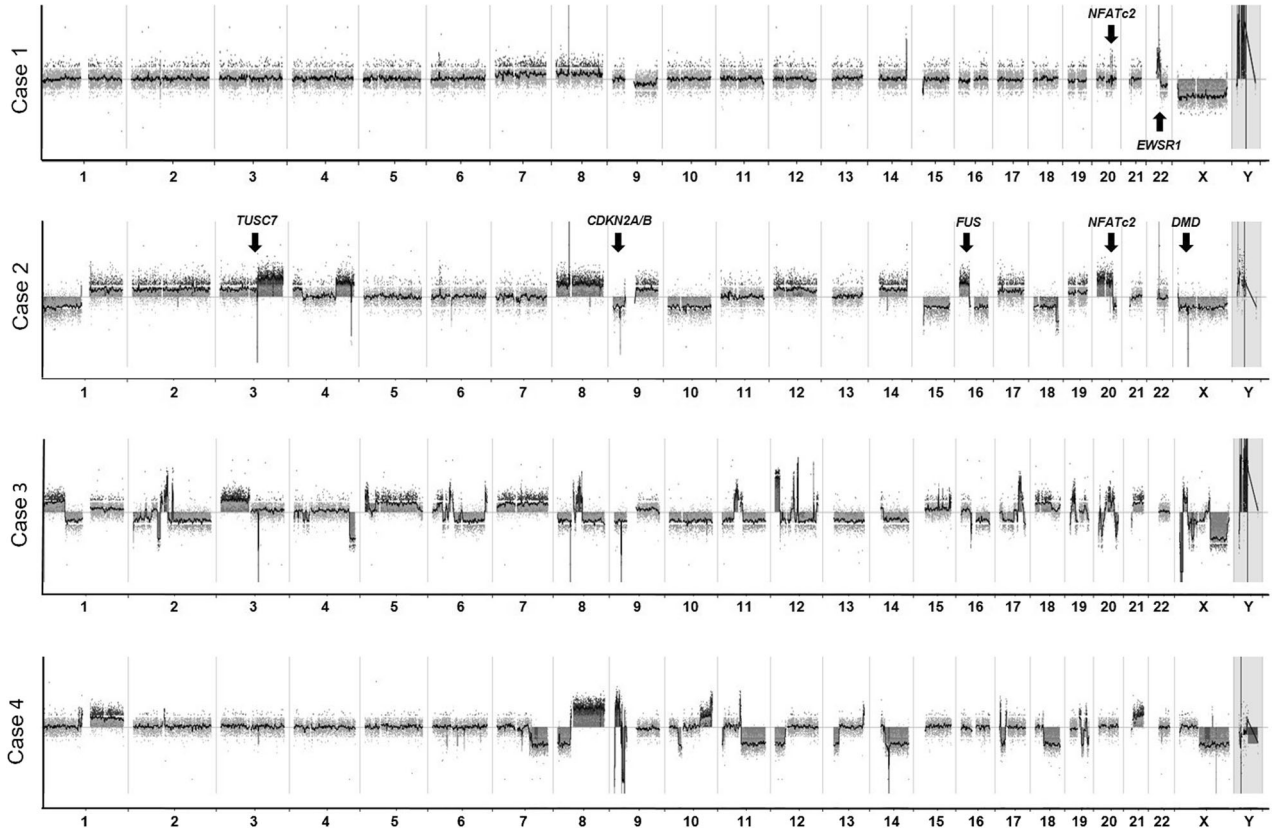

Fig. 5 Array-based Comparative Genomic Hybridization profiles of *NFATc2*-Sarcomas. Chromosomes 1 to X/Y are plotted on the x-axis and copy number alterations on the y-axis. Supplemental Material.

features are common, to date, only four tumor-related deaths have been confirmed. This finding may be due to the relatively short follow-up periods (<24 months) in half of the published cases. However, whether *NFATc2*-Sarcoma is less lethal than ES, cannot be currently excluded. Another important point is that the response to neoadjuvant chemotherapy has been suboptimal (<90% necrosis) in most reported cases of *NFATc2*-Sarcoma [3–5, 17, 21, 22]. Our results are in line with these findings and support the idea that they are poorly sensitive to chemotherapy, especially to ES and osteosarcoma chemotherapy regimens.

Histologically, *NFATc2*-Sarcoma shows a predominant component of small to medium-sized round cells, which tend to have more irregular nuclei than the ones seen in ES. In general, cells grow in lobules and sheets, but trabecular and corded growth patterns (rarely seen in other round cell sarcomas) can be present. In addition, variable amounts of extracellular matrix are frequently seen. The type of matrix is variable and has been previously characterized as collagenous, sclerotic, hyaline, myxoid, myxohyaline, and chondromyxoid [3–5, 15, 16]. When considered together, these morphological features resemble the ones described in the "Ewing-like" family of tumors, particularly in *CIC*-Rearranged Sarcomas. As previously reported, nuclear pleomorphism can be seen in *NFATc2*-sarcomas, albeit rarely [3, 17]. This feature is rare in translocation derived sarcomas and has been suggested to be induced by neoadjuvant chemotherapy [17]. However, in our study, only 1/2 cases with pleomorphic nuclei received neoadjuvant treatment, supporting that this can be an intrinsic property of these tumors. A curious finding was the presence of an abundant collagenous matrix simulating osteoid in one case from our series. As depicted, this feature may be deceiving both in biopsy and resection specimens where the diagnosis of a neoplasm with osteogenic differentiation could be favored. Nevertheless, SATB2 was negative (Fig. 3e) and the collagenous matrix seen in our case was fibrillary, a feature rarely seen in osteoid. Of note, although rare, neoplastic bone formation has been reported in three previous cases of *NFATc2*-Sarcoma [15, 17, 23] and this feature led to the initial misdiagnosis of two cases as an aggressive osteoblastoma [23] and as an ossifying fibromyxoid tumor [15]. Cartilaginous differentiation, a unique finding reported in our study, may also prompt a wrong diagnosis of a chondrogenic/osteogenic tumor, which further stresses the difficulty in recognizing these tumors based on morphological grounds alone. In this context, it should be emphasized that contrarily to *NFATc2*-Sarcomas, osteosarcomas and chondrosarcomas do not show recurrent gene fusions. Taking into account these facts, we believe that molecular

studies should be considered in any bone neoplasm with a round cell component and cartilaginous or osseous differentiation, particularly if arising in young male adults. This systematic approach will be helpful for correctly classifying *NFATc2*-Sarcomas and for identifying their full morphological spectrum.

Immunohistochemical assessment with markers commonly used in the characterization of small round cell tumors showed variable expression in the studied cases. Although CD99 was ubiquitously expressed, diffuse membranous staining, as classically seen in ES, was only demonstrated in 3/7 cases. Other positive markers, included: ETV-4, WT1, BCOR, Pan-Keratin, ERG, and PS100. ETV-4 and WT1 are frequently used in the screening of round cell sarcoma to triage for *CIC-S*arcoma [29], where, contrary to *NFATc2*-Sarcoma, they are expressed strongly and diffusely. BCOR is a sensitive but unspecific marker that along with CCNB3 is expressed diffusely in most *BCOR-CCNB3* Sarcomas [30, 31]. More importantly, this type of BCOR staining was not seen in the tested cases of *NFATc2*-Sarcoma. Pan-Keratin staining can be seen in round cell sarcomas, including ES [32] and *CIC*-Sarcomas [33]. Moreover, epithelial marker expression (pan-keratin and EMA) has also been reported in previous cases of *NFATc2*-sarcoma [3, 4], indicating that this is a frequent finding. ERG is variably expressed in different tumor subtypes, including most cases of ES with ERG fusions [34] were, in general, stains diffusely. As others and we [3, 34] have shown, ERG staining can be present in *NFATc2*-Sarcoma but is typically focal and weak in intensity. PS100 was focally positive in the cartilaginous areas seen in two cases of our series but was completely negative in the round cells of all tested cases. This feature is a helpful hint for ruling out myoepithelial neoplasms, which can be morphologically similar to *NFATc2*-Sarcoma. Lastly, the absence of diffuse expression of Desmin and SATB2 in *NFATc2*-sarcomas is against a diagnosis of rhabdomyosarcoma and round cell osteosarcoma, respectively. Of note, recently, Yoshida et al. [15] reported a consistent expression of NKX3-1 in 9/11 cases of *EWSR1* variants of *NFATc2*-Sarcomas, suggesting a diagnostic utility of this marker. In this regard, our results indicate that NKX3-1 polyclonal antibodies should be privileged as we did not see staining using monoclonal antibodies. Additional studies are warranted.

An important finding of our study is the utility of AGGRECAN immunohistochemistry for the identification of *NFATc2*-Sarcoma. AGGRECAN is a 2316 aminoacids-long protein coded by *ACAN*, which represents the major proteoglycan in the cartilaginous tissue [35]. Structurally, it is composed of three globular domains (G1-G3) and three extended domains (IGD, KS, and CS). The globular domains mediate cell adhesion, chondrocyte apoptosis, and interaction between chondrocyte and matrix. The extended domains contain proteolytic cleavage sites and keratin sulfate and chondroitin sulfate binding domains. While the importance of AGGRECAN in the pathogenesis of arthropathies is well documented [36], its role in cancer remains poorly characterized. Previous studies have used its expression as a surrogate marker of cartilaginous differentiation [37], and its transcriptional expression has been documented both in the central nervous system [38] and in notochordal cells [39]. The present results indicate that AGGRECAN is a sensitive and specific marker of *NFATc2*-Sarcoma due to its limited expression in the control group of round cell sarcomas. Nevertheless, it is important to remark that AGGRECAN was diffusely positive in around one fourth of the tested cases of mesenchymal chondrosarcoma and in a single case of *CIC*-Sarcoma. Hence, its expression should be interpreted with caution and in conjunction with a panel of antibodies when molecular or cytogenetic studies are not used for diagnostic confirmation. In addition, a subset of myoepitheliomas and myoepithelial carcinomas showed diffuse AGGRECAN expression. This peculiar finding contributes to the debate of whether *NFATc2*-sarcomas are linked with myoepithelial neoplasms with which they share morphological [4] and cytogenetic [40, 41] features but seem to differ at the transcriptome level [8]. Despite the exceptions mentioned above, our results indicate that in an adequate clinical and morphological setting, AGGRECAN could have an important role in the detection of *NFATc2*-sarcomas.

NFATc2-Sarcomas are distinctive as they represent the first example of a human neoplasm driven by a translocation involving *NFATc2* [2]. This gene's product acts as a transcription factor implicated in the regulation of cytokine expression in T lymphocytes [42] and plays a role in cancer migration and invasion [43, 44]. Moreover, the components of the *NFAT* family of transcription factors are attractive candidates for target therapy due to their implication in cancer development and progression [45]. Notably, *NFATc2* also regulates the expression of chondrocyte-specific genes and bone formation [46, 47]. Its ablation in mice cartilage induces osteoarthritis along with loss of proteoglycans, including AGGRECAN. The latter makes us speculate that *NFATc2* deregulation may lead to AGGRECAN overexpression and eventually to chondroid metaplasia and osteoid formation in a subset of *NFATc2*-sarcomas. Importantly, most reported cases of *NFATc2*-Sarcoma harbor *EWSR1* rearrangements and gains/amplifications which when present may serve as a diagnostic hint [2–5]. This particular abnormality generally affects the 5′ end of the gene and can be reliably identified with commercially available FISH *EWSR1* break-apart assays (Fig. 4f). In this regard, it is worth mentioning that to date,

only a single reported case of soft tissue myoepithelioma showed amplification of *EWSR1*, but this was limited to the 3′ end of the gene [40].

In our study, aCGH analysis was performed on four cases of *NFATc2*-Sarcoma. The cases with *FUS-NFATc2* fusions showed very complex genomic profiles contrasting with the simpler profile of a case with an *ESWR1-NFATc2* fusion. Genomic complexity was objectified by the determination of the GI, which is calculated by assessing the number and type of DNA copy number alterations. Notably, the presence of a higher GI has been correlated with a worse patient outcome in several soft tissue neoplasms [13, 14]. This was confirmed in our study, as all *FUS-NFATc2* cases were clinically aggressive. Another interesting finding was that *FUS-NFATc2* cases harbored recurrent deletions of tumor suppressor genes, including *CDKN2A/B*, *TUSC7*, and *DMD*. In this regard, it is notable that *CDKN2A* deletions are correlated with a worse prognosis in a subset of soft tissue sarcomas [48]. Similarly, deletions of *TUSC7* are associated with poor survival in osteosarcoma patients [49], likely due to the promotion of cancer cell proliferation [50]. Lastly, deletions of *DMD* have been associated with tumor progression in myogenic sarcomas due to the loss of Dystrophin, which inhibits sarcoma cell migration, invasion, and anchorage-independent growth [51]. Interestingly, segmental chromosomal gains covering the fusion genes were detected in both *EWSR1* and *FUS* variants, supporting that these anomalies are not restricted to *EWSR1-NFATc2* cases. On the other hand, 9q deletions, reported in most *EWSR1-NFATc2* variants [2, 6], were absent in all tested *FUS* cases. Further, gains of chromosome 8, frequently described in ES [52], were seen in both fusion variants. Altogether, our findings suggest that *FUS-NFATc2* tumors show frequent deletions of tumor suppressor genes and more complex karyotypes than *EWSR1-NFATc2* tumors. Furthermore, both variants can harbor fusion gene gains.

Taking into account current and previous results, a question that needs to be further addressed is whether *FUS-NFATc2* and *EWSR1-NFATc2* tumors should be grouped. Initial studies using independent clustering analysis of RNA sequencing data from frozen material suggested that these tumors had different transcriptomic profiles [8]. Nevertheless, this was inconsistent in our RNA sequencing data from FFPE material (Supplemental Material). Indeed, when compared with a reduced subgroup of round cell sarcomas, *NFATc2*-Sarcomas formed a tight cluster, independent of the fusion partner involved and distinct from ES (Supplemental Material). This discrepancy is not surprising, considering that the determination of distinct tumor clusters is influenced by several variables, including: total number of cases in the analyzed cohort, interrelationship among cases, and the clustering patterns of the different tumor subgroups. Due to these discordant results, it is currently difficult to assure (based solely on molecular grounds) whether these fusion variants should be separated and considered as independent entities. Still, when integrating the morphological features of all studied tumors, it is notable that *FUS-NFATc2* variants were prone to show cartilaginous areas and presented more atypia, necrosis, and mitotic activity. Also, these cases were clinically aggressive, and some genomic alterations varied from the ones previously characterized in *EWSR1-NFATc2* tumors [2, 6]. Interestingly, AGGRECAN staining did not differ among fusion variants, and the markers differentially expressed in the *FUS-NFATc2* cases from our series (Table 3) have all been previously reported in *EWSR1-NFATc2* tumors [3, 20, 29, 34]. Overall, our results argue for considering *FUS-NFATc2* variants as a distinct aggressive subgroup of *NFATc2*-sarcomas. However, future larger studies with adequate clinical, morphological, and molecular data are needed to confirm or reject this hypothesis.

In summary, we have described a series of seven cases of *NFATc2*-sarcomas, highlighting that they are distinctive round cell tumors, mostly affecting the bones of young males and consistently expressing AGGRECAN. These neoplasms show significant differences with ES, including limited response to neoadjuvant chemotherapy, morphological findings, and genomic and transcriptomic profiles. Furthermore, correct subclassification of *FUS* and *EWSR1* fusion variants is warranted due to potentially different biological behavior. Altogether, our results support the development of more adapted treatment strategies for *NFATc2*-Sarcoma and provide a useful diagnostic tool for the identification of this rare sarcoma subtype.

Acknowledgements We want to thank Dr Sabrina Croce, Jessica Massiere, and Flora Rebier for their assistance. This work was supported by a grant from the charity "Au Fil d'Oriane."

Compliance with ethical standards

Conflict of interest The authors declare that they have no conflict of interest.

Publisher's note Springer Nature remains neutral with regard to jurisdictional claims in published maps and institutional affiliations.

References

1. Le Loarer F, Pissaloux D, Coindre JM, Tirode F, Vince DR. Update on families of round cell sarcomas other than classical ewing sarcomas. Surg Pathol Clin. 2017;10:587–620.
2. Szuhai K, Ijszenga M, de Jong D, Karseladze A, Tanke HJ, Hogendoorn PC. The NFATc2 gene is involved in a novel cloned translocation in a ewing sarcoma variant that couples its function in immunology to oncology. Clin Cancer Res. 2009;15:2259–68.
3. Wang GY, Thomas DG, Davis JL, Ng T, Patel RM, Harms PW, et al. EWSR1-NFATC2 translocation-associated sarcoma clinicopathologic findings in a rare aggressive primary bone or soft

tissue tumor. Am J Surg Pathol. 2019. https://doi.org/10.1097/PAS.0000000000001260.
4. Bode-Lesniewska B, Fritz C, Exner GU, Wagner U, Fuchs B. EWSR1-NFATC2 and FUS-NFATC2 gene fusion-associated mesenchymal tumors: clinicopathologic correlation and literature review. Sarcoma 2019;2019:9386390.
5. Diaz-Perez JA, Nielsen GP, Antonescu C, Taylor MS, Lozano-Calderon SA, Rosenberg AE. EWSR1/FUS - NFATc2 rearranged round cell sarcoma: clinicopathological series of 4 cases and literature review. Hum Pathol. 2019. https://doi.org/10.1016/j.humpath.2019.05.001.
6. Koelsche C, Kriegsmann M, Kommoss FKF, Stichel D, Kriegsmann K, Vokuhl C, et al. DNA methylation profiling distinguishes Ewing-like sarcoma with EWSR1–NFATc2 fusion from Ewing sarcoma. J Cancer Res Clin Oncol. 2019;145:1273–81.
7. Kovar H, Amatruda J, Brunet E, Burdach S, Cidre-Aranaz F, de Alava E, et al. The second European interdisciplinary Ewing sarcoma research summit-A joint effort to deconstructing the multiple layers of a complex disease. Oncotarget. 2016;7:8613–24.
8. Watson S, Perrin V, Guillemot D, Reynaud S, Coindre JM, Karanian M, et al. Transcriptomic definition of molecular subgroups of small round cell sarcomas. J Pathol. 2018;245:29–40.
9. Baldauf MC, Orth MF, Dallmayer M, Marchetto A, Gerke JS, Rubio RA, et al. Robust diagnosis of Ewing sarcoma by immunohistochemical detection of super-enhancer-driven EWSR1-ETS targets. Oncotarget 2017;9:1587–601.
10. Le Loarer F, Cleven AHG, Bouvier C, Castex MP, Romagosa C, Moreau A, et al. A subset of epithelioid and spindle cell rhabdomyosarcomas is associated with TFCP2 fusions and common ALK upregulation. Mod Pathol. 2020;33:404–19.
11. Bray NL, Pimentel H, Melsted P, Pachter L. Near-optimal probabilistic RNA-seq quantification. Nat Biotechnol. 2016;34:525–7.
12. Wilkerson MD, Hayes DN. ConsensusClusterPlus: a class discovery tool with confidence assessments and item tracking. Bioinformatics. 2010;26:1572–3.
13. Croce S, Ducoulombier A, Ribeiro A, Lesluyes T, Noel JC, Amant F, et al. Genome profiling is an efficient tool to avoid the STUMP classification of uterine smooth muscle lesions: acomprehensive array-genomic hybridization analysis of 77 tumors. Mod Pathol. 2018;31:816–28.
14. Lagarde P, Pérot G, Kauffmann A, Brulard C, Dapremont V, Hostein I, et al. Mitotic checkpoints and chromosome instability are strong predictors of clinical outcome in gastrointestinal stromal tumors. Clin Cancer Res. 2012;18:826–38.
15. Yoshida KI, Machado I, Motoi T, Parafioriti A, Lacambra M, Ichikawa H, et al. NKX3-1 is a useful immunohistochemical marker of EWSR1-NFATC2 sarcoma and mesenchymal chondrosarcoma. Am J Surg Pathol. 2020. https://doi.org/10.1097/PAS.0000000000001441 [Epub ahead of print].
16. Mantilla JG, Ricciotti RW, Chen E, Hoch BL, Liu YJ. Detecting disease-defining gene fusions in unclassified round cell sarcomas using anchored multiplex PCR/targeted RNA next-generation sequencing—Molecular and clinicopathological characterization of 16 cases. Genes Chromosom Cancer. 2019. https://doi.org/10.1002/gcc.22763.
17. Yau DTW, Chan JKC, Bao S, Zheng Z, Lau GTC, Chan ACL. Bone sarcoma with EWSR1-NFATC2 fusion: sarcoma with varied morphology and amplification of fusion gene distinct from ewing sarcoma. Int J Surg Pathol. 2019. https://doi.org/10.1177/1066896919827093.
18. Toki S, Wakai S, Sekimizu M, Mori T, Ichikawa H, Kawai A, et al. PAX7 immunohistochemical evaluation of Ewing sarcoma and other small round cell tumours. Histopathology. 2018;73:645–52.
19. Antonescu C. Round cell sarcomas beyond Ewing: emerging entities. Histopathology. 2014;64:26–37.
20. Machado I, Yoshida A, Morales MGN, Abrahão-Machado LF, Navarro S, Cruz J, et al. Review with novel markers facilitates precise categorization of 41 cases of diagnostically challenging, "undifferentiated small round cell tumors". A clinicopathologic, immunophenotypic and molecular analysis. Ann Diagn Pathol. 2018;34:1–12.
21. Cohen JN, Sabnis AJ, Krings G, Cho SJ, Horvai AE, Davis JL. EWSR1-NFATC2 gene fusion in a soft tissue tumor with epithelioid round cell morphology and abundant stroma: a case report and review of the literature. Hum Pathol. 2018;81:281–90.
22. Kinkor Z, Vaneček T, Svajdler M Jr, Mukenšnabl P, Veselý K, Baxa J, et al. Where does Ewing sarcoma end and begin - two cases of unusual bone tumors with t(20;22)(EWSR1-NFATc2) alteration. Cesk Patol. 2014;50:87–91.
23. Sadri N, Barroeta J, Pack SD, Abdullaev Z, Chatterjee B, Puthiyaveettil R, et al. Malignant round cell tumor of bone with EWSR1-NFATC2 gene fusion. Virchows Arch. 2014;465:233–9.
24. Romeo S, Bovée JV, Kroon HM, Tirabosco R, Natali C, Zanatta L, et al. Malignant fibrous histiocytoma and fibrosarcoma of bone: a re-assessment in the light of currently employed morphological, immunohistochemical and molecular approaches. Virchows Arch. 2012;461:561–70.
25. Brohl AS, Solomon DA, Chang W, Wang J, Song Y, Sindiri S, et al. The genomic landscape of the Ewing Sarcoma family of tumors reveals recurrent STAG2 mutation. PLoS Genet. 2014;10:e1004475.
26. Bacci G, Ferrari S, Bertoni F, Rimondini S, Longhi A, Bacchini P, et al. Prognostic factors in nonmetastatic ewing's sarcoma of bone treated with adjuvant chemotherapy: analysis of 359 patients at the Istituto Ortopedico Rizzoli. J Clin Oncol. 2000;18:4–4.
27. Stahl M, Ranft A, Paulussen M, Bölling T, Vieth V, Bielack S, et al. Risk of recurrence and survival after relapse in patients with Ewing sarcoma. Pediatr Blood Cancer. 2011;57:549–53.
28. Leavey PJ, Collier AB. Ewing sarcoma: prognostic criteria, outcomes and future treatment. Expert Rev Anticancer Ther. 2008;8:617–24.
29. Hung YP, Fletcher CD, Hornick JL. Evaluation of ETV4 and WT1 expression in CIC-rearranged sarcomas and histologic mimics. Mod Pathol. 2016;29:1324–34.
30. Kao YC, Sung YS, Zhang L, Jungbluth AA, Huang SC, Argani P, et al. BCOR overexpression is a highly sensitive marker in round cell sarcomas with BCOR genetic abnormalities. Am J Surg Pathol. 2016;40:1670–8.
31. Cohen-Gogo S, Cellier C, Coindre JM, Mosseri V, Pierron G, Guillemet C, et al. Ewing-like sarcomas with BCOR-CCNB3 fusion transcript: a clinical, radiological and pathological retrospective study from the Société Française des Cancers de L'Enfant. Pediatr Blood Cancer. 2014;61:2191–8.
32. Srivastava A, Rosenberg AE, Selig M, Rubin BP, Nielsen GP. Keratin-positive ewing's sarcoma: an ultrastructural study of 12 cases. Int J Surg Pathol. 2005;13:43–50.
33. Antonescu CR, Owosho AA, Zhang L, Chen S, Deniz K, Huryn JM, et al. Sarcomas with cic-rearrangements are a distinct pathologic entity with aggressive outcome: a clinicopathologic and molecular study of 115 cases. Am J Surg Pathol. 2017;41:941–9.
34. Wang WL, Patel NR, Caragea M, Hogendoorn PC, López-Terrada D, Hornick JL, et al. Expression of ERG, an Ets family transcription factor, identifies ERG-rearranged Ewing sarcoma. Mod Pathol. 2012;25:1378–83.
35. Kiani C, Chen L, Wu YJ, Yee AJ, Yang BB. Structure and function of aggrecan. Cell Res. 2002;12:19–32.
36. Roughley PJ, Mort JS. The role of aggrecan in normal and osteoarthritic cartilage. J Exp Orthop. 2014;1:8.
37. Aigner T, Oliveira AM, Nascimento AG. Extraskeletal myxoid chondrosarcomas do not show a chondrocytic phenotype. Mod Pathol. 2004;17:214–21.

38. Domowicz MS, Sanders TA, Ragsdale CW, Schwartz NB. Aggrecan is expressed by embryonic brain glia and regulates astrocyte development. Dev Biol. 2008;315:114–24.
39. Sandell LJ. In situ expression of collagen and proteoglycan genes in notochord and during skeletal development and growth. Microsc Res Tech. 1994;28:470–82.
40. Antonescu CR, Zhang L, Chang NE, Pawel BR, Travis W, Katabi N, et al. EWSR1-POU5F1 fusion in soft tissue myoepithelial tumors. A molecular analysis of sixty-six cases, including soft tissue, bone, and visceral lesions, showing common involvement of the EWSR1 gene. Genes Chromosom Cancer. 2010;49:1114–24.
41. Huang SC, Chen HW, Zhang L, Sung YS, Agaram NP, Davis M, et al. Novel FUS-KLF17 and EWSR1-KLF17 fusions in myoepithelial tumors. Genes Chromosom Cancer. 2015;54:267–75.
42. Macian F. NFAT proteins: key regulators of T-cell development and function. Nat Rev Immunol. 2005;5:472–84.
43. Xiao ZJ, Liu J, Wang SQ, Zhu Y, Gao XY, Tin VP, et al. NFATc2 enhances tumor-initiating phenotypes through the NFATc2/SOX2/ALDH axis in lung adenocarcinoma. ELife. 2017;6:e26733.
44. Kim GC, Kwon HK, Lee CG, Verma R, Rudra D, Kim T, et al. Upregulation of Ets1 expression by NFATc2 and NFKB1/RELA promotes breast cancer cell invasiveness. Oncogenesis 2018;7:91.
45. Qin JJ, Nag S, Wang W, Zhou J, Zhang WD, Wang H, et al. NFAT as cancer target: mission possible? Biochim Biophys Acta. 2014;1846:297–311.
46. Greenblatt MB, Ritter SY, Wright J, Tsang K, Hu D, Glimcher LH, et al. NFATc1 and NFATc2 repress spontaneous osteoarthritis. Proc Natl Acad Sci. 2013;110:19914–9.
47. Koga T, Matsui Y, Asagiri M, Kodama T, de Crombrugghe B, Nakashima K, et al. NFAT and Osterix cooperatively regulate bone formation. Nat Med. 2005;11:880–5.
48. Bui N, Przybyl J, Million L, Van De Rijn M, Ganjoo KN. CDKN2A deletion as a prognostic marker: a clinico-genomic analysis of sarcoma patients. J Clin Oncol. 2018;15:11543–11543.
49. Pasic I, Shlien A, Durbin AD, Stavropoulos DJ, Baskin B, Ray PN, et al. Recurrent focal copy-number changes and loss of heterozygosity implicate two noncoding RNAs and one tumor suppressor gene at chromosome 3q13.31 in osteosarcoma. Cancer Res. 2010;70:160–71.
50. Cong M, Li J, Jing R, Li Z. Long non-coding RNA tumor suppressor candidate 7 functions as a tumor suppressor and inhibits proliferation in osteosarcoma. Tumour Biol. 2016;37:9441–50.
51. Wang Y, Marino-Enriquez A, Bennett RR, Zhu M, Shen Y, Eilers G, et al. Dystrophin is a tumor suppressor in human cancers with myogenic programs. Nat Genet. 2014;46:601–6.
52. Grünewald TGP, Cidre-Aranaz F, Surdez D, Tomazou EM, de Álava E, Kovar H, et al. Ewing sarcoma. Nat Rev Dis Prim. 2018;4:5.

Affiliations

Raul Perret[1] · Julien Escuriol[1,2] · Valérie Velasco[1] · Laetitia Mayeur[1] · Isabelle Soubeyran[1,3] · Christophe Delfour[4] · Sébastien Aubert[5] · Marc Polivka[6] · Marie Karanian[7,8] · Alexandra Meurgey[7] · Sophie Le Guellec[9] · Noelle Weingertner[10] · Sylvia Hoeller[11] · Jean-Michel Coindre[1,2] · Frédérique Larousserie[12] · Gaëlle Pierron[13] · Franck Tirode[8] · François Le Loarer[1,2,3]

[1] Department of Biopathology, Bergonie Institute, Bordeaux, France

[2] Bordeaux University, Talence, France

[3] INSERM U1218, ACTION Unit, Bordeaux, France

[4] Department of Pathology, Montpellier University Hospital, Montpellier, France

[5] Department of Pathology, Institut de Pathologie, Univ. Lille, CHU Lille, F-59000 Lille, France

[6] Department of Pathology, APHP, Hôpital Cochin, DMU Imagina, Université de Paris, F-75014 Paris, France

[7] Department of Pathology, Leon Berard Center, Lyon, France

[8] Univ Lyon, Université Claude Bernard Lyon 1, INSERM 1052, CNRS 5286, Centre Léon Bérard, Cancer Research Center of Lyon, Lyon, France

[9] Department of Pathology, Claudius Regaud Institute, Toulouse-Oncopole, Toulouse, France

[10] Department of Pathology, Strasbourg Regional University Hospital (Hautepierre Hospital), Strasbourg, France

[11] Department of Pathology, Hospital of the University of Basel, Basel, Switzerland

[12] Department of Pathology, APHP-Cochin Hospital, Paris, France

[13] Department of Tumor Biology, Curie Institute, Paris, France